Full title: **Zika virus-like particles bearing covalent dimer of envelope protein protect mice from lethal challenge**

Short title: **Zika virus vaccine exposing E protein dimers**

Giuditta De Lorenzo[1†], Rapeepat Tandavanitj[1†], Jennifer Doig[1], Chayanee Setthapramote[1,3], Monica Poggianella[2], Ricardo Sanchez Velazquez[1], Hannah E. Scales[4], Julia M. Edgar[4], Alain Kohl[1], James Brewer[4], Oscar R. Burrone[2], Arvind H. Patel[1*].

[1] *MRC - University of Glasgow Centre for Virus Research, G61 1QH, Glasgow, Scotland, UK*

[2] *Molecular immunology Group, International Centre for Genetic Engineering and Biotechnology, 34149, Trieste, Italy*

[3] *Department of Clinical Pathology, Faculty of Medicine Vajira Hospital , Navamindradhiraj University, Bangkok, 10300, Thailand*

[4] *University of Glasgow, Institute of Infection, Immunity and Inflammation, University Place, G12 8TA, Glasgow, Scotland, UK.*

*Corresponding author: Arvind.patel@glasgow.ac.uk

[†] Giuditta De Lorenzo, Rapeepat Tandavanitj contributed equally to this work. Author order was determined on the basis of seniority.

Abstract

Zika virus (ZIKV) envelope (E) protein is the major target of neutralizing antibodies in infected host, and thus represents a candidate of interest for vaccine design. However, a major concern in the development of vaccines against ZIKV and the related dengue virus is the induction of cross-reactive poorly neutralizing antibodies

that can cause antibody-dependent enhancement (ADE) of infection. This risk necessitates particular care in vaccine design. Specifically, the engineered immunogens should have their cross-reactive epitopes masked, and they should be optimized for eliciting virus-specific strongly neutralizing antibodies upon vaccination. Here, we developed ZIKV subunit- and virus-like particle (VLP)-based vaccines displaying E in its wild type form, or E locked in a covalently linked dimeric (cvD) conformation to enhance the exposure of E dimers to the immune system. Compared with their wild-type derivatives, cvD immunogens elicited antibody with higher capacity of neutralizing virus infection of cultured cells. More importantly, these immunogens protected animals from lethal challenge with both the African and Asian lineages of ZIKV, impairing virus dissemination to brain and sexual organs. Moreover, the locked conformation of E reduced the exposure of epitopes recognized by cross-reactive antibodies and therefore showed a lower potential to induce ADE *in vitro*. Our data demonstrated a higher efficacy of the VLPs in comparison with the soluble dimer and support VLP-cvD as a promising ZIKV vaccine.

Author Summary

Infection with Zika virus (ZIKV) leads to the production by host of antibodies that target the viral surface envelope (E) protein. A subset of these antibodies can inhibit virus infection, thus making E as a suitable candidate for the development of vaccine against the virus. However, the anti-ZIKV E antibodies can cross-react with the E protein of the related dengue virus on account of the high level of similarity exhibited by the two viral proteins. Such a scenario may lead to severe dengue disease.

Therefore, the design of a ZIKV vaccine requires particular care. Here, we tested two candidate vaccines containing a recombinant form of the ZIKV E protein that is forced in a covalently stable dimeric conformation (cvD). They were generated with an explicit aim to reduce the exposure of the cross-reactive epitopes. One vaccine is composed of a soluble form of the E protein (sE-cvD), the other is a more complex virus-like particle (VLP-cvD). We used the two candidate vaccines to immunize mice and later infected with ZIKV. The animals produced high level of inhibitory antibodies and were protected from the infection. The VLP-cvD was the most effective and we believe it represents a promising ZIKV vaccine candidate.

Introduction

For decades Zika virus (ZIKV) was largely ignored as a human pathogen but the recent epidemic in South America has brought to light neurological complications (i.e. Guillain-Barré syndrome)(1) and congenital Zika syndrome (i.e. microcephaly and other malformations)(2) making ZIKV a public health threat in affected countries. ZIKV infection occurs mainly via mosquito bite but its persistence in bodily fluids like semen allows sexual transmission (3). There is currently no vaccine or treatment available, making their development a priority in ZIKV research.

Current approaches to vaccine development include purified inactivated virus (4), DNA/RNA/vector-based vaccines encoding structural proteins (5-10) and purified viral-like particles (VLPs) (11, 12) or protein subunits (13, 14). Some of these candidates are currently undergoing phase 1 of clinical trial but the design of a successful ZIKV vaccine is complicated by the close relation of ZIKV with other

flaviviruses and especially dengue virus (DENV), also transmitted by *Aedes* mosquito vectors and overlapping across many areas.

ZIKV genome, like other members of the *Flaviviridae* family, is composed of a positive strand RNA encoding a single polyprotein that is cleaved into structural (capsid, precursor-membrane and envelope) and non-structural proteins (NS1, NS2, NS3, NS4 and NS5). The envelope (E) glycoprotein, with its three domains (DI, DII and DIII), is the main target of the host immune response (15). During the initial stages of flavivirus genesis, the E protein is associated with the precursor-membrane protein (prM) and assumes a trimeric conformation; only during the passage in the trans-Golgi network, where the viral particle encounters an acidic environment, the trimers dissociate to re-assemble as dimers (16). This new conformation is necessary to allow furin-mediated cleavage of prM into pr and M generating a mature E dimer (17). Once released in the extracellular environment, pr dissociates and the particle becomes infectious. During infection, the low pH of the endosome triggers a new conformational modification that mediates fusion of viral and endosomal membranes (18). However, the particle maturation process is often incomplete releasing a viral progeny partially displaying E protein in trimers containing prM. In addition, E protein is in continuous dynamic motion, a phenomenon called “virus breathing” that is strain- and temperature-dependent (19). These two factors - incomplete maturation and viral breathing - have important consequences on epitope accessibility. At its tip, DII harbours the fusion loop (FL) represented by an amino acid sequence that is highly conserved among flaviviruses. FL is masked by DI and DIII when E protein on the virion is in a dimeric form but becomes exposed upon re-arrangement of E in the acidic endosome following cell

entry. Epitopes located on DI/DII, especially in the FL region (FLE), are immuno-dominant but recognized by cross-reactive and poorly neutralizing antibodies (20, 21). This class of antibodies can be responsible for antibody-dependent enhancement (ADE) of infection where antibody-bound virus particles are endocytosed via the Fcγ receptor, leading to a more severe infection (22). Antibodies to prM also contribute to ADE (22).

In addition, the most potent neutralizing antibodies often recognize complex quaternary epitopes than bind to multiple adjacent E proteins, epitopes that are available only when the E protein is assembled in a viral particle and therefore could not be elicited upon immunization with subunits (23). Recently, a new class of quaternary epitopes, called the Envelope Dimer Epitopes (EDE), have been described (24). EDE epitopes are displayed when the E proteins form a head-to-tail dimeric conformation. Highly neutralizing antibodies recognizing EDE were discovered in the sera of DENV-infected patients but interestingly, they were also shown to efficiently neutralize ZIKV, both in *in vitro* and in *in vivo* experiments (25-27). Upon binding to pre-fusion E dimers, these antibodies can prevent the transition of E to a trimeric form and consequently abrogate membrane fusion and infection.

Here, we aimed to develop antigens for ZIKV vaccination that can drive the immune response preferentially against quaternary/complex epitopes, to increase the neutralizing potential. Our recent study demonstrated that the introduction of a disulphide bridge by A264C substitution can stabilize E in a covalent dimer (cvD) conformation (28). This structure reduces the exposure of the unwanted FLE in favour of EDE. We generated cvD forms of a soluble E (sE-cvD) and a virus-like particle (VLP-cvD). The latter is expected to present E predominantly in form of dimers, conferring a smooth surface to the particles. Vaccination of mice with these

antigens afforded full protection from lethal ZIKV challenge. Moreover, in comparison to their WT counterparts, the cvD immunogens elicited antibodies that exhibited lower *in vitro* ADE of DENV, yellow fever virus (YFV) and West Nile virus (WNV). Our data confirmed the potential of cvD mutation in generating an immune response against neutralizing conformational epitopes, and further identified VLP-cvD as the most promising candidate of the two cvD derivatives tested.

Results

Design, expression and purification of E covalent dimer-based vaccines: We focused on designing antigens that would elicit antibodies to the complex quaternary epitopes that span two or more ZIKV E molecules. Immunogens based on EDE have a great potential, but a stable dimeric conformation of E is not easy to achieve. For this reason, we used a strategy of generating a covalently stable dimeric form by introducing Ala to Cys mutation in DII (A264C) of E as described previously (28). The stable dimeric E generated is thus expected to enhance exposure of EDE and reduce presentation of the unwanted immune-dominant FL region in DII to the immune system.

We generated a V5 epitope-tagged soluble ZIKV E (sE; i.e. E lacking its stem and membrane anchor domains) in its wild-type form (sE-WT), and in the form of a covalently stabilised dimer (sE-cvD) containing the A264C mutation (Fig 1A) (28). In addition, we also generated wild type (WT) and cvD forms of ZIKV virus-like particles (VLPs) using plasmid constructs encoding the capsid anchor region (Ca) followed by the full-length prM and E (Fig 1C). These proteins were produced by transient transfection of Expi293F cells with the relevant constructs and subsequently purified

148 from the cell medium as described in Methods. The purified sE proteins were
149 analysed in SDS-PAGE gel under reducing and non-reducing conditions (Fig 1B). As
150 expected, the sE-WT was visible exclusively in the monomeric form, with an
151 apparent molecular weight of ~50 kDa, while sE-cvD under non-reducing conditions
152 had an apparent molecular weight corresponding to a dimer (~110 kDa) that could
153 be reduced to a monomer upon incubation with DTT. A small amount of sE-cvD was
154 seen in a monomeric form under non-reducing condition. VLPs were expressed in a
155 similar fashion and purified as shown in Fig 1C. SDS-PAGE and western blot
156 analysis confirmed the presence of dimeric E in VLP-cvD (~110 kDa) when analysed
157 under non-reducing conditions, and this was reduced to a monomer in the presence
158 of DTT (Fig 1D). We also observed two additional minor bands: one in the non-
159 reducing gel where a higher molecular weight protein possibly representing a more
160 complex aggregate of E, and an approximately 90 kDa protein in the reducing gel
161 which is likely an intermediate product resulting from an incomplete thiol reduction. In
162 contrast, monomeric E (~55 kDa) was found in the VLP-WT preparation under both
163 reducing and non-reducing conditions. The molecular weight of E in the VLP
164 preparations was higher than that of the two sE proteins (Fig 1B) on account of the
165 presence of the stem and anchor sequences. As expected, the viral M (10 kDa) was
166 also detected in both forms of VLPs. Protein M is the product of furin-mediated
167 cleavage of prM (25 kDa) during maturation of virus particles. The presence of M
168 protein in the absence of prM suggested that in VLP-cvD the mutated glycoprotein
169 underwent a complete maturation process during its synthesis, yielding smooth
170 particles bearing the cvD E protein. Instead, the VLP-WT preparation contained
171 residual prM implying that they were not fully matured (Fig 1E). Electron micrographs

(Fig 1F) of both types of VLPs showed particles of around 50 nm comparable to the size of infectious ZIKV particles (29).

Antibodies generated by cvD immunogens are conformation-sensitive: ZIKV cannot infect immuno-competent mice due to its inability to counteract murine interferon response (30). We therefore used the interferon receptor-deficient transgenic knock-out (*Ifnar1*$^{-/-}$) A129 mice, which are susceptible to ZIKV infection and which have been shown to be amenable to vaccine evaluation studies (31). A cohort each of 4 weeks-old mixed male and female animals (n=6) were vaccinated with sE-WT, sE-cvD, VLP-WT, VLP-cvD, or PBS (as control). Three doses of 10 µg (sEs) or 2 µg (VLPs) of protein adjuvanted with ALUM (1%) combined with MPLA (5 µg) were administered by sub-cutaneous route as shown in Fig 2A. One week after the last dose, blood samples were tested for the presence of anti-E antibodies.

We first tested the serum antibodies for binding to biotinylated derivatives of ZIKV sE proteins fused in-frame with the Biotin-Acceptor Peptide (BAP). Specifically, recombinant sE-WT-BAP (monomer) or sE-cvD-BAP (dimer) co-expressed with the bacterial biotin ligase BirA (32, 33) (to allow *in vivo* mono-biotinylation) were used to quantify the titre of antibodies recognizing E in its monomeric or dimeric form.

A comparison of the binding levels showed that sE-cvD immunisation elicited antibodies titres against the dimer four times higher than those obtained with sE-WT. On the other hand, analysis of the sera from VLP-WT- and VLP-cvD-vaccinated animals by ELISA showed no significant changes in the levels of antibodies (Fig 2C). It should be noted that this ELISA format is not robust enough to discriminate antibodies binding to more complex epitopes.

196 In order to further characterise the types of antibodies elicited by our cvD antigens,
197 we used a recently developed cytofluorimetry assay of cells displaying dimers of
198 ZIKV sE protein (paper in submission). In this assay, the C-terminus of sE is fused to
199 the trans-membrane and cytosolic tail of the type-I trans-membrane protein MHC-Iα
200 for plasma membrane display of the protein, as previously reported (28). This assay
201 has the potential to discriminate antibodies binding exclusively to dimeric E on the
202 basis of the pH-dependent mobility of E protein: at pH7, that resembles the neutral
203 extracellular environment, the protein is in a dimeric conformation but at pH6,
204 mimicking the conformational changes that occur in the acidic endosome vesicles
205 during infection, it moves to a pre-fusion monomeric conformation. When exposed to
206 a neutral pH (pH7), E can physiologically dimerize, and therefore be recognized by
207 the dimer specific monoclonal antibody EDE 1C10 (24). However, this interaction is
208 completely abrogated when cells are exposed to a lower pH (pH6), due to the
209 disruption of the dimer. Thus, with this dimer-specific antibody two populations of
210 cells can be detected by flow cytometry – antibody-bound and unbound – depending
211 on the assay conditions (Fig 3A - EDE). On the other hand, antibodies binding to
212 epitopes that do not require dimeric conformation of the protein are poorly affected
213 by the pH and therefore show no differences in the binding capacity, as shown using
214 in-house made monoclonal antibody DIII-1B (Fig 3A – DIII-1B), that recognizes a
215 linear epitope located on domain III (Figs 3E and F). This assay is primarily
216 designed, and indeed works optimally, for monoclonal antibodies. Nevertheless, we
217 reasoned that it would still be useful in evaluating the nature of antibodies in sera
218 from vaccinees containing a mix of IgGs capable of binding to linear or
219 conformational epitopes. As shown in Figs 3B to 3D, serum antibodies from sE-WT-
220 and VLP-WT-immunized groups seemed to not be particularly affected in the binding

by the pH-dependent change of conformation. In contrast, sera from sE-cvD- and VLP-cvD-vaccinated animals showed a more consistent pH-dependent difference in the relative peak positions (Fig 3B to 3D).

Taken together, the data suggest that cvD antigens elicited a population of antibodies more sensitive to changes in conformation then the one elicited by the WT immunisation.

cvD antigens elicit neutralizing antibodies in mice: A new immunisation was performed using the same procedure shown in Fig 2A. Antibody titres were measured using exclusively the sE-cvD-BAP ELISA (Fig 4A). The neutralizing capacity of these sera was then determined in a micro-neutralization (MN) assay that we had previously developed (9). This sandwich ELISA accurately measures the levels of glycoprotein E in infected cells thus enabling quantitation of virus infectivity. Vero cells were infected with the Puerto Rican ZIKV strain PRVABC59 (an Asian lineage isolate) that had been pre-incubated for 1 hour with serially diluted mouse sera. Three days post-infection the level of cellular E protein was determined by sandwich ELISA. Percentage of infectivity was calculated relative to E yield in cells infected in absence of sera. As shown in Fig 4B, antibodies elicited by sE-cvD and VLP-cvD significantly neutralized virus infection compared to sera from control group. VLP-cvD sera neutralized more strongly than sE-WT sera. Although not statistically significant, we observed a trend towards higher *in vitro* neutralization titres from cvD-elicited sera than their WT counterparts (Fig 4B).

cvD immunogens protect mice from ZIKV challenge: To assess *in vivo* efficacy of our candidate vaccines, we challenged the above immunized animals with 10^4 pfu of ZIKV PRVABC59 by subcutaneous injection as shown in Fig 5A. , A scoring system was used to monitor the progress of the disease, based on severity of clinical signs and symptoms, as described in Fig 5D. A score of 3 was considered as the humane endpoint. Animals were monitored for 9 days for their body weight changes (Fig 5C) and clinical signs (Fig 5E). The PBS control group began losing weight at 4 days post-challenge (dpc) and subsequently exhibited clinical signs of infection and were euthanized at 7-8 dpc (Figs. 5B and C, grey lines). The sE-WT group lost less weight but exhibited clinical signs comparable to those seen in the PBS control group albeit with delayed kinetics (Figs. 5B and C, orange lines). One mouse of the sE-WT group succumbed to infection. A similar profile of weight change, clinical scores and survival were observed in VLP-WT group (Figs. 5B and C red lines) compared to the sE-WT group. Importantly, all animals immunised with cvD antigens survived the challenge, maintained a more stable weight profile and showed rapid recovery from the clinical signs of infection (Figs. 5B and C, purple and blue lines). Viremia was determined by RT-qPCR on blood samples taken at days 2, 3, 4 and 7 during the course of the challenge (Figs. 6A and B). Since the limit of the assay was determined as a titre of 10^2 pfu equivalent/mL, for statistical analysis this value was given to all the samples that were below the limit of detection. As expected, PBS control mice showed very high viremia (>10^6 pfu/mL) which peaked at 3 dpc. In contrast, in all vaccinated animals the viremia peaked at 4 dpc, although the levels varied. Specifically, the sE-WT-vaccinated animals displayed levels comparable to those observed in the PBS control group (>10^5 pfu equivalent/mL). Instead, consistent reduction in viremia levels was observed in VLP-WT-, sE-cvD- and VLP-

cvD-vaccinated animals which in the latter two groups was significant. In particular, the geometric mean of viral titre of 4×10^2 pfu equivalent/mL was the lowest in VLP-cvD-vaccinated group. Relative organ viral load was analysed by RT-qPCR of viral RNA extracted from brain, spleen and sex organs, which were collected immediately after euthanasia (Fig 6C). ΔΔCT method was used to calculate the titre relative to an average of PBS control group. Although all four antigens reduced brain viral load, only cvD antigens reduced that of the sex organs. In case of spleen viral transmission, sE-cvD and VLP-cvD were better than sE-WT and control group whereas VLP-WT was only better than control group. All together, these data confirmed the unsuitability of wild-type antigens (especially sE-WT) whereas both cvD derivatives conferred full protection against ZIKV infection *in vivo*.

cvD reduces *in vitro* ADE: Due to the close relationship with DENV and other mosquito-borne flaviviruses, a ZIKV vaccine is very likely to elicit cross-reactive antibodies that may fail in neutralizing other flavivirus infection and instead lead to a worse disease outcome. Our candidate vaccines are designed in order to reduce this risk, limiting exposure of highly cross-reactive but low cross-neutralising epitopes in favour of broadly neutralizing ones. We performed an *in vitro* ADE assays using the K562 monocyte cell line that expresses the Fcγ-receptor. Infection of these cells doesn't occur through the normal entry pathway. Rather, it occurs exclusively via Fcγ-receptor-mediated internalization of the antibody-bound virus. In keeping with this, we observed an extremely low infection rate in absence of antibodies binding to the virus, i.e. when the virus was pre-incubated in the absence of serum (data not shown) or in the presence of the sera from our PBS-injected mice. Viruses pre-incubated with ten-fold serial dilutions of the sera were added to the cells, incubated

for three days, and then analysed to determine the percentage of infection by cytofluorimetry. Experiment was performed in triplicate. (Fig 7).

We used ZIKV as a control in the assay. As expected, pre-incubation with all the sera gave the same pattern of infection, suggesting that antibodies (neutralizing or otherwise) in the four groups of sera bind to ZIKV similarly to mediate infection. This is not surprising, since internalization occurs independently of the normal receptors and therefore the neutralizing antibodies are no longer capable of blocking entry. When tested against the four DENV serotypes, YFV and WNV, sera from the sE-WT immunized group conferred infection of between 50% and 100% of cells. Instead, 10 times lower levels of infection were observed with sE-cvD sera, suggesting the presence of a much lower level of cross-reacting antibodies in these sera. Similarly, sera from VLP-cvD-immunised mice exhibited a 10-fold reduced infectivity compared to sera from VLP-WT animals. Particularly interesting was the level of infected cells obtained after virus incubation with VLP-WT sera, which was significantly higher than the infection obtained following incubation of the virus with the sera from sE-cVD and VLP-cvD immunised animals. These results suggest that the covalent dimer-based E vaccines (both, sE-cvD and VLP-cvD) confer a lower risk of ADE in comparison to their WT counterparts as determined by this experimental model.

VLP-cvD protection coverage includes ZIKV African lineage: ZIKV has diverged decades ago into two lineages, the African and the Asian. Where the Asian lineage is responsible for the last epidemics and is linked to neurological outcomes and birth-defects, the African lineage is -intriguingly- well known to be more pathogenic in *in vivo* models (34). Since a safe ZIKV vaccine should guarantee coverage of both

318 African and Asian lineages, we tested the VLP-cvD protectivity upon infection with a
319 Ugandan (MP1751) isolate of ZIKV. Immunization and challenge were performed as
320 previously described (Figs 2A and 5A). The PBS group lost weight starting from day
321 3 post-challenge and all mice reached the endpoint at day 6 (Figs 8A and B, grey
322 lines. Fig 8C). VLP-cvD-vaccinated group instead showed a stable body weight and
323 all animal survived the challenge (Figs 8A and B, blue lines. Fig 8C). PBS-
324 immunised-control mice showed high peak of viremia (>10^7 pfu/mL) at 4 dpc while
325 the vaccinated mice showed a highly significant reduction in viremia (~10^2 pfu/mL)
326 (Fig 8D). Also, virus dissemination to the brain was suppressed in the VLP-cvD
327 immunized mice (Fig 8E). All together, these results confirm the broadly protective
328 potential of our vaccine candidate.
329

330 ## Discussion

331 Monoclonal antibodies recognizing quaternary epitopes that span on more than one
332 E protein are reported to be the most neutralizing and cross-reactive class of
333 antibodies (24, 35, 36). Nevertheless, they constitute only a minority of the
334 antibodies elicited by a natural infection, where the larger response focuses on
335 poorly neutralizing and cross-reactive epitopes located on DI/DII (15, 37). The
336 incomplete maturation of particles and the mobility of E reduce their exposure,
337 especially to dimeric epitopes, in favour of the Fusion-Loop epitope. However, our
338 vaccines are designed in order to lock E in a dimeric conformation, impairing its
339 disassembly and forcing the protein to display the desired epitopes.
340

341 E-homodimer stability was proved several times to be affected by temperature:
342 dimerization is favoured at 28˚C and reduced at 37°C, hence physiological

temperature is another element that contributes to impair dimers exposure to the immune system (38). But 28˚C is also a crucial temperature for expression and secretion of E protein, both in the soluble form but also as part of VLPs (28). Since this temperature is not compatible with genetic vaccination approaches, in which DNA or RNA encoding the antigen is administered and the antigen is then produced by the host cells at physiological temperature, the full potential of our antigens as candidate vaccines was evaluated in a protein-based vaccination approach.

Recently, a characterization of two dimeric E antigens was published, dimerization was achieved by the A264C mutation or replacing the E transmembrane domain with the FC fragment of a human IgG (39). While this manuscript was under preparation, two other articles reported development and evaluation of dimer-based subunit vaccines similar to that described in here (40, 41). The authors showed that in all three cases the antigens were able to induce in mice the production of neutralizing antibodies. However, our work is the first application of E covalent dimers to virus-like particles that proved in our hands to be a vaccine candidate superior to the soluble dimer.

We tested the potential of E covalent-dimers when expressed in the form of soluble protein, lacking the stem-anchor, and also as VLP. In comparison with sE-WT we observed a dramatic effect of the cvD mutation on the immune response, with a drastic reduction of antibodies binding to monomeric E and an impressive increase in protective activity upon lethal challenge. When the comparison was performed with the VLPs, the effect was less dramatic in terms of anti-dimer antibody titres. This is likely due to the thermal stability of dimers that is higher in ZIKV than in DENV (42),

ZIKV E dimers are more stable, as already proven by the necessity of a double disulphide bridge to lock DENV E dimer when one bridge is sufficient in ZIKV E. In addition, our ELISA and binding assays are based on E subunits presented in a monomeric or dimeric form but cannot fully recreate the complex symmetry of E protein on the viral particles therefore cannot quantify the contribution of antibodies binding to adjacent dimers. However, the difference in antibody response and protectivity was enough to achieve an important reduction in DENV ADE. In this regard it is noteworthy that the VLP-cvD lacked prM indicating their complete maturation. In contrast, VLP-WT contained prM that can elicit anti-prM antibodies upon vaccination. The prM protein is naturally present in DENV or ZIKV particles, due to incomplete maturation, but prM antibodies from DENV patients showed no or poor neutralizing activity and may instead likely induce ADE (43). All together these observations strongly suggest that covalently linked E dimer can bring even higher benefits to the development of a DENV vaccine.

The development of a ZIKV vaccine requires attention to the possible cross-reaction with DENV. ADE of infection between different DENV serotypes is widely recognised as the cause of dengue shock syndrome (DSS) but the role that ZIKV infection may play at any point in influencing DENV infections is still unclear. Unfortunately, it is not easy to experimentally predict ADE, since results obtained from *in vitro* and *in vivo* settings, and those from among different *in vivo* models are not always consistent. So far animal models have not been able to replicate the full repertoire of the antibody response in humans. In addition, it is difficult to reproduce severe DENV infection in animal models; in most cases the severity of infection is based on increased viremia in the infected animals. *In vitro* tests performed with DENV-

393 positive sera or DENV monoclonal antibodies showed cross-reactivity and ADE of
394 ZIKV infection, similar to experiments performed in mouse models (20, 44-46).
395 Conversely, analysis performed in non-human primate models ruled out a negative
396 effect of previous DENV exposure on ZIKV infection (47), which was later confirmed
397 by population studies with asymptomatic ZIKV infection in subjects positive for DENV
398 antibodies (48). Concerns of cross-reaction and ADE were also raised about
399 vaccination against other flaviviruses. *In vitro* studies supported negligible risk of
400 ADE of ZIKV after tick-borne encephalitis virus vaccination and no clinical evidence
401 of increased disease severity in vaccinated people has emerged so far (49). The fear
402 of predisposing vaccinated individual to DSS generated a reluctance to deploy the
403 YFV vaccine in DENV endemic areas, but a recent long-term study showed no
404 evidence of increased risk (50). Not much is known about the role of WNV antibodies
405 in causing other flavivirus ADE and vice versa. Like DENV, sera from WNV patients
406 exhibit *in vitro* ADE of ZIKV (45). However, while DENV ADE is a well-documented
407 phenomenon, to our knowledge there is as yet no evidence of ADE occurring
408 between DENV/ZIKV and WNV in humans.
409 However, the sequence homology between ZIKV and DENV is high with elevated
410 antibody cross-reactivity (15, 20). According to a recent publication, ZIKV infection
411 can increase risk of a severe DENV2 disease at the same level as a previous
412 heterologous dengue infection (51) and therefore how ZIKV vaccination can affect
413 DENV pathogenesis is a pertinent question that remains to be addressed.
414
415 We evaluated the ADE potential (on DENV, YFV and WNV) of the different sera
416 using K562 cells. These cells express high levels of FcγRIIA and significantly favour
417 FcγR-mediated infection, making them suitable for studying ADE in an *in vitro*

418 setting. We found that sera from sE-WT-immunised animals exhibited high ADE in
419 our assay presumably because the antigen exposes well known conserved epitopes,
420 such as the FLE, allowing high level of cross-reactivity. In contrast, ADE was
421 strongly reduced when E was locked in the dimeric form (sE-cvD) and properly
422 folded, likely because conserved but poorly neutralising epitopes on DI/DII are not
423 exposed. We obtained interesting results upon comparison of sera from mice
424 immunised with VLPs bearing a WT or a cvD form of the full-length ZIKV E
425 glycoprotein. While the VLP-WT conferred protection from lethal infection in mice,
426 the sera from the same immunised animals induced *in vitro* ADE of ZIKV at levels
427 comparable to sE-WT-immunised sera, or even higher as in the case of DENV1 and
428 DENV4. In contrast, and as with sE-CvD, sera from VLP-cvD-immunised animals
429 exhibited strongly reduced ADE of the flavivirus under analysis. This raises safety
430 concerns about a vaccine that, despite protecting from ZIKV infection, may bring
431 more adverse effects on subsequent DENV infections. Once again, this risk is
432 reduced with the VLP-cvD antigen. However, to what extent ADE *in vitro* mimics any
433 *in vivo* effects remains to be determined.
434
435 ADE of DENV upon ZIKV immunisation is a risk that cannot be underestimated. One
436 way to reduce antibody cross-reactivity would be to focus on developing a less
437 conserved subunit vaccine, like DIII. However, we recently showed that this
438 approach fails in protecting from *in vivo* challenges(52). The development of
439 engineered, safe vaccine is probably an essential requirement to tackle this
440 concerning public health challenge. Our two immunogens proved the high potential
441 of engineered E protein locked in a dimeric conformation as a suitable vaccine

candidate, with the most promising results achieved when the protein is part of a structurally more complex antigen presented in the form of a virus-like particle.

Material and Methods

Cell lines and virus strains: Expi293F (Thermo Fisher Scientific) embryonic human kidney adapted to serum-free conditions) cells were grown in Expi293™ Expression Medium as per the manufacturers' protocol. Vero E6 cells were grown in Dulbecco's Modified Eagle's Medium (DMEM) (Life Technologies) containing 10% fetal bovine serum (FBS) (Life Technologies) and penicillin-streptomycin (Gibco), K562 cells were grown in Roswell Park Memorial Institute (RPMI) 1640 medium (Life Technologies) containing 10% Fetal Bovine Serum (FBS) (Life Technologies). ZIKV PRVABC59 (kindly supplied by BEI Resources; Accession Number KX087101) and ZIKV MP1751 (005V-02871; kindly supplied by Public Health England: Accession Number KY288905.1) were used for infection experiments, micro-neutralisation and animal challenge.

Plasmid DNA constructs: ZIKV sE-encoding sequence (codon 1-404) was amplified from ArD158095 strain (Accession number KF383121.1) as described in Sloan Campos et al[28]. sE fused to a N-terminal immunoglobulin leader sequence (sec) and a C-terminal V5 tag (GKPIPNPLLFLD) was cloned into a pVax vector. A mammalian codon-optimized ZIKV prME gene sequence, flanked by the C-terminal portion of C and the N-terminal reside of NS1, was obtained from ZIKV PE243 Brazilian strain (Accession number KX197192.1[53]) (aa 105-815 of the polyprotein) and cloned into a pDIs vector. The A264C mutation was introduced by site-directed mutagenesis into both plasmids.

Protein expression and purification: sE-WT, sE-cvD, VLP-WT and VLP-cvD were expressed using ExpiFectamine™ 293 Transfection Kit (Thermo Fisher Scientific) following manufacturer's instructions. After 16 hours, cells were moved to 28°C. At 5 days post-transfection the supernatant was harvested and filtered. sE proteins were purified using the V5-tagged Protein Purification Gel (Caltag Medsystems Ltd) eluting with 2 mg/mL of V5 peptide. VLPs, they were pelleted down by ultracentrifugation (115,000 g, 4°C, 2 hours) (Sorvall discovery 90SE with Surespin630 rotor) through a cushion of 20% sucrose in TN Buffer (20 mM Tris and 120 mM NaCl). The pellet was re-suspended in TN buffer and loaded on discontinuous density gradient made by sodium potassium tartrate and glycerol in TN buffer (29). Tartrate concentration ranged from 10 to 30% with interval of 5% whilst that of glycerol ranged from 7.5 to 22.5% with interval of 3.75%. After centrifugation (Sorvall discovery 90SE with TH641 rotor) at 175,000 g, 4°C, 2 hours, fractions were collected and analysed for the presence of ZIKV E by western lot. ZIKV E protein-positive fractions were pooled, dialysed against Dulbecco's phosphate-buffered saline (DPBS) (Life Technologies) and concentrated using spin column (Amicon® Ultra-15 (100 kDa), Merck Millipore) before being subjected to size-exclusion chromatography. Briefly, ~500 µL of concentrated pooled fractions was loaded onto HiPrep 16/60 Sephacryl S-500 HR column (GE Healthcare) then 1.5 column volume of mobile phase (DPBS) was run through the column at flow rate of 0.5 mL/min using the AKTA Pure (GE Healthcare) system. Fractions were collected and tested for ZIKV E protein. Positive fractions were pooled and concentrated using the Amicon® Ultra-15 (100 kDa; Merck Millipore) spin column.

491 The concentration of the purified proteins was determined using NanodropOne
492 (ThermoScietific).
493
494 **SDS-PAGE and western blot:** sE samples were subjected to 10% SDS-PAGE, and
495 the fractionated proteins detected by direct staining of the gel with InstantBlue
496 (Sigma) or by western blot. VLP samples were separated by 10% or 14% SDS-
497 PAGE later blotted to PVDF membrane (Immobilon®-FL, Merck Millipore) and
498 blocked overnight with ODYSSEY® blocking buffer, LI-COR then incubated DIII1B
499 antibody (anti-ZIKV E DIII generated in-house as described in Figure 3) or ZIKA prM
500 antibody (GeneTex) for 1 hour followed by anti-mouse IgG (IRDye® 800CW, LI-
501 COR) and anti-rabbit IgG (IRDye® 680RD, LI-COR). Images were acquired by
502 LICOR machine.
503
504 **Electron microscopy:** VLPs were adsorbed for 3 min to Formvar carbon films
505 mounted on 400 mesh per inch copper grids (Agar Scientific). Samples were washed
506 three times with distilled water and stained with 2% saturated uranylacetate (Agar
507 Scientific) for 2 min at room temperature. Specimens were analysed in a
508 transmission electron microscope (JEM-1200 EX II, JEOL) equipped with a CCD
509 camera (Orius, Gatan) at an acceleration voltage of 80 kV.
510
511 **Animal immunisation:** Four-week old male and female *Ifnar1*$^{-/-}$ mice (A129, 129S7
512 background; Marshall BioResources) (n=6) were subcutaneously immunised with
513 ZIKV antigen formulated in aluminium hydroxide gel (1% ALUM, Brenntag) combined
514 with 5 µg monophosphoryl lipid A (MPLA)(InvivoGen) or PBS containing the
515 adjuvant. Purified sE antigens used in each immunisation contained 10 µg protein

whilst it was 2 µg in case of VLPs. Mice were immunised at 0, 2 and 3 weeks and bled 4 weeks after primary immunisation for antibody titration and micro-neutralisation assay. Four weeks after primary immunisation, mice were challenged subcutaneously with 10^4 pfu of Puerto Rican ZIKV (PRVABC59) or Uganda ZIKV (MP1751). Blood was collected at 2, 3, 4 and 7 dpc and 10 µL of sera were assessed by RT-qPCR. Mice were euthanised when they exhibited three or more signs of moderate severity or lost more than 15% body weight, otherwise 9/10 days after challenge.

Animal Ethics

All animal research described in this study was approved by the University of Glasgow Animal Welfare and Ethical Board and was carried out under United Kingdom Home Office Licenses, P9722FD8E, in accordance with the approved guidelines and under the UK Home Office Animals (Scientific Procedures) Act 1986 (ASPA).

ELISA: Recombinant biotinylated proteins (sE, sE-cvD and DIII) were expressed at 28°C using ExpiFectamine™ 293 Transfection Kit (Thermo Fisher Scientific). Cell supernatant was harvested and dialyzed. Biotinylated proteins were captured in ELISA plates pre-coated with 5 µg/mL of Avidin (Sigma) in Na_2CO_3/$NaHCO_3$ buffer pH 9.6, subsequently blocked with PBS containing 0.05% Tween-20 and 1% bovine serum albumin (BSA-Sigma). Serial dilutions of mouse sera were tested for binding to the biotinylated proteins and the bound antibodies detected using HRP-conjugated anti-mouse IgG A4416 (Sigma) and TMB substrate (Life Technologies).

Antibody binding assay: This assay was performed as previously described in (paper in submission). HEK cells stably expressing ZIKV sE protein on the surface were blocked in 1% BSA in PBS at pH 6 or 7 and then incubated with mouse sera diluted 1:500 in the same solution. After wash, cells were incubated with secondary anti-mouse Alexa 488 (Jackson Immunoresearch) 1:50000 in 1% BSA PBS pH 7 and analysed by cytofluorimetry in a FACSCalibur (BD Biosciences).

Micro-neutralisation (MN) assay: This assay was performed as described in Lopez-Camacho et al (9). Briefly, 7×10^3/well of Vero cells were seeded in 96-well plates and incubated at 37 °C in 5% CO_2. Next day, three-fold serially diluted mice sera were first incubated at 37°C for 1 hour with 100 pfu/well ZIKV strain PRVABC57. The serum/virus mix was then used to infect cells. After 1 hour of incubation at 37 °C, 100 µL of medium was added to each well. At day 3 post-infection, cells were lysed in lysis buffer (20 mM Tris-HCl [pH 7.4], 20 mM iodoacetamide, 150 mM NaCl, 1 mM EDTA, 0.5% Triton X-100 and Complete protease inhibitors) and the viral E protein quantitated by sandwich ELISA (see below). The amount of E protein detected correlates with the level of virus infectivity which was presented as % of ZIKV infectivity relative to the control (i.e., virus not pre-incubated with immune sera). The MN_{50} titre was defined as the serum dilution that neutralised ZIKV infection by 50%.

Sandwich ELISA to assess ZIKV infectivity: ELISA plates were coated with 3 µg/mL of purified pan-flavivirus MAb D1-4G2-4-15 (ATCC® HB112TM) in PBS and incubated overnight at RT and subsequently blocked for 2 hours at RT with PBS containing 0.05% Tween-20 and 2% skimmed milk powder. After washing with

PBST, ZIKV-infected cell lysates were added and incubated for 1 hour at RT. Wells were washed with PBST, incubated with anti-ZIKV E polyclonal R34 IgG (9) at 6 µg/ml in PBST for 1 hour at RT and washed again. Antibodies bound to ZIKV envelope protein were detected using HRP conjugate anti-rabbit IgG 7090 (Abcam) and TMB substrate (Life Technologies).

Quantitation of viral RNA by RT-qPCR: Viral RNA was extracted from 10 µL of mouse sera using QIAamp® viral RNA Mini Kit (Qiagen) or about 20 mg of organs homogenised by Precellys Lysing Kit Hard tissue grinding (Bertin Technologies) using RNeasy viral mini kit. The viral load was measured by RT-qPCR using One-Step SYBR® Primescript™ RT-PCR kit II (Takara). CT values of serum samples were used to calculate serum viral titre according to regression equation built by RNA extracted from 10 µL of 10^2-10^6 pfu/mL of ZIKV (PRVABC59 or MP1751). In case of relative organ viral load, CT values of ZIKV gene and internal control B2M gene were used for calculating ΔCT values. Average ΔCT of PBS-injected mice was used as reference to calculate ΔΔCT value. Primers pair for PRVABC59 ZIKV gene was Forward:5'-GTTGTCGCTGCTGAAATGGA-3' and Reverse:5'-GGGGACTCTGATTGGCTGTA-3'. Primers pair for MP1751 ZIKV gene was Forward:5'-ACTTCCGGTGCGTTACATGA-3' and Reverse:5'-GGGCTTCATCCATGATGTAG-3'. Primers pair for the B2M genes was Forward: 5'-CGGCCTGTATGCTATCCAGA-3' Reverse: 5'- GGGTGAATTCAGTGTGAGCC -3'.

ADE assay: Ten-fold serial dilutions of pooled sera were mixed with $4x10^3$ pfu of each virus and incubated for 1.5 hour at 37 °C before mixing with $4x10^4$ K562 cells. After incubation at 37°C for 2 days (for WNV) or 3 days (all other viruses), cells were

fixed with 2% PFA for 30 min and then washed in PBS. Blocking and permeabilization buffer (0.1% saponine, 2 % FBS, 0.1% NaN_3 in PBS) was added to cell for 30 min at 4 °C. Cells are incubated with mAb 4G2 (1 µg/mL) for 1hour at 4 °C followed by secondary anti-mouse Alexa 488 (Jackson Immunoresearch, 1:50000). After washing with PBS, cells are re-suspended in blocking buffer without saponine and analysed by cytofluorimetry in a FACSCalibur (BD Biosciences).

Statistical analysis: Normality was determined by Ryan-Joiner Normality test with Minitab Software. Statistical analysis was done as indicated in figure legends, with Minitab or GraphPad Prims softwares. *p<0.05, **p<0.01, ***p<0.001. Where asterisks are missing the differences are calculated as nonsignificant (ns).

Acknowledgment

We thank Marion McElwee and James Streetley for help with imaging VLPs by electron microscopy. We acknowledge the provision of ZIKV strains PRVABC59 and MP1751 (005V-02871) by BEI Resources and Public Health England/EVAg, respectively. This research is funded by the Department of Health and Social Care using UK Aid funding and is managed by the NIHR (AHP and AK); the UK Medical Research Council (MC_UU12014/2 and MC_UU_12014/8) (AHP and AK). The views expressed in this publication are those of the author(s) and not necessarily those of the Department of Health and Social Care. This project was also partially funded through the European Union's Horizon 2020 research and innovation programme under ZikaPLAN grant agreement No 734584 (JME). The funders had no role in study design, data collection and analysis, decision to publish, or preparation of the manuscript.

Author contribution

The CVR has adopted the CRediT taxonomy (https://casrai.org/credit/). Authors' contribution is as follows. GDL: conceptualization, data curation, formal analysis, investigation, project administration, methodology, supervision, validation, visualization, writing - original draft, writing - review & editing; RT: data curation, formal analysis, investigation, validation, visualization, writing – original draft, writing review & editing; JD: data curation, investigation, writing - review & editing; CS: investigation, visualization, writing - review & editing; MP: investigation, methodology, validation, writing - review & editing; RS: investigation, writing - review & editing; HES: resources, writing - review & editing; JME: resources, writing - review & editing; AK: funding acquisition, resources, writing - review & editing; JB: resources, writing - review & editing; ORB: conceptualization, resources, writing - original draft, writing - review & editing, AHP: conceptualization, funding acquisition, project administration, resources, supervision, writing - original draft, writing - review & editing.

Competing interests

The authors declare no competing interests.

References

1. Munoz LS, Barreras P, Pardo CA. 2016. Zika Virus-Associated Neurological Disease in the Adult: Guillain-Barre Syndrome, Encephalitis, and Myelitis. Semin Reprod Med 34:273-279.
2. Mlakar J, Korva M, Tul N, Popovic M, Poljsak-Prijatelj M, Mraz J, Kolenc M, Resman Rus K, Vesnaver Vipotnik T, Fabjan Vodusek V, Vizjak A, Pizem J, Petrovec M, Avsic Zupanc T. 2016. Zika Virus Associated with Microcephaly. N Engl J Med 374:951-8.
3. D'Ortenzio E, Matheron S, Yazdanpanah Y, de Lamballerie X, Hubert B, Piorkowski G, Maquart M, Descamps D, Damond F, Leparc-Goffart I. 2016. Evidence of Sexual Transmission of Zika Virus. N Engl J Med 374:2195-8.

4. Abbink P, Larocca RA, De La Barrera RA, Bricault CA, Moseley ET, Boyd M, Kirilova M, Li Z, Ng'ang'a D, Nanayakkara O, Nityanandam R, Mercado NB, Borducchi EN, Agarwal A, Brinkman AL, Cabral C, Chandrashekar A, Giglio PB, Jetton D, Jimenez J, Lee BC, Mojta S, Molloy K, Shetty M, Neubauer GH, Stephenson KE, Peron JP, Zanotto PM, Misamore J, Finneyfrock B, Lewis MG, Alter G, Modjarrad K, Jarman RG, Eckels KH, Michael NL, Thomas SJ, Barouch DH. 2016. Protective efficacy of multiple vaccine platforms against Zika virus challenge in rhesus monkeys. Science 353:1129-32.
5. Chahal JS, Fang T, Woodham AW, Khan OF, Ling J, Anderson DG, Ploegh HL. 2017. An RNA nanoparticle vaccine against Zika virus elicits antibody and CD8+ T cell responses in a mouse model. Sci Rep 7:252.
6. Dowd KA, Ko SY, Morabito KM, Yang ES, Pelc RS, DeMaso CR, Castilho LR, Abbink P, Boyd M, Nityanandam R, Gordon DN, Gallagher JR, Chen X, Todd JP, Tsybovsky Y, Harris A, Huang YS, Higgs S, Vanlandingham DL, Andersen H, Lewis MG, De La Barrera R, Eckels KH, Jarman RG, Nason MC, Barouch DH, Roederer M, Kong WP, Mascola JR, Pierson TC, Graham BS. 2016. Rapid development of a DNA vaccine for Zika virus. Science 354:237-240.
7. Larocca RA, Abbink P, Peron JP, Zanotto PM, Iampietro MJ, Badamchi-Zadeh A, Boyd M, Ng'ang'a D, Kirilova M, Nityanandam R, Mercado NB, Li Z, Moseley ET, Bricault CA, Borducchi EN, Giglio PB, Jetton D, Neubauer G, Nkolola JP, Maxfield LF, De La Barrera RA, Jarman RG, Eckels KH, Michael NL, Thomas SJ, Barouch DH. 2016. Vaccine protection against Zika virus from Brazil. Nature 536:474-8.
8. Pardi N, Hogan MJ, Pelc RS, Muramatsu H, Andersen H, DeMaso CR, Dowd KA, Sutherland LL, Scearce RM, Parks R, Wagner W, Granados A, Greenhouse J, Walker M, Willis E, Yu JS, McGee CE, Sempowski GD, Mui BL, Tam YK, Huang YJ, Vanlandingham D, Holmes VM, Balachandran H, Sahu S, Lifton M, Higgs S, Hensley SE, Madden TD, Hope MJ, Kariko K, Santra S, Graham BS, Lewis MG, Pierson TC, Haynes BF, Weissman D. 2017. Zika virus protection by a single low-dose nucleoside-modified mRNA vaccination. Nature 543:248-251.
9. Lopez-Camacho C, Abbink P, Larocca RA, Dejnirattisai W, Boyd M, Badamchi-Zadeh A, Wallace ZR, Doig J, Velazquez RS, Neto RDL, Coelho DF, Kim YC, Donald CL, Owsianka A, De Lorenzo G, Kohl A, Gilbert SC, Dorrell L, Mongkolsapaya J, Patel AH, Screaton GR, Barouch DH, Hill AVS, Reyes-Sandoval A. 2018. Rational Zika vaccine design via the modulation of antigen membrane anchors in chimpanzee adenoviral vectors. Nat Commun 9:2441.
10. Griffin BD, Muthumani K, Warner BM, Majer A, Hagan M, Audet J, Stein DR, Ranadheera C, Racine T, De La Vega MA, Piret J, Kucas S, Tran KN, Frost KL, De Graff C, Soule G, Scharikow L, Scott J, McTavish G, Smid V, Park YK, Maslow JN, Sardesai NY, Kim JJ, Yao XJ, Bello A, Lindsay R, Boivin G, Booth SA, Kobasa D, Embury-Hyatt C, Safronetz D, Weiner DB, Kobinger GP. 2017. DNA vaccination protects mice against Zika virus-induced damage to the testes. Nat Commun 8:15743.
11. Boigard H, Alimova A, Martin GR, Katz A, Gottlieb P, Galarza JM. 2017. Zika virus-like particle (VLP) based vaccine. PLoS Negl Trop Dis 11:e0005608.
12. Garg H, Sedano M, Plata G, Punke EB, Joshi A. 2017. Development of Virus like Particle Vaccine and Reporter Assay for Zika Virus. J Virol doi:10.1128/JVI.00834-17.
13. Han JF, Qiu Y, Yu JY, Wang HJ, Deng YQ, Li XF, Zhao H, Sun HX, Qin CF. 2017. Immunization with truncated envelope protein of Zika virus induces protective immune response in mice. Sci Rep 7:10047.
14. Liang H, Yang R, Liu Z, Li M, Liu H, Jin X. 2018. Recombinant Zika virus envelope protein elicited protective immunity against Zika virus in immunocompetent mice. PLoS One 13:e0194860.
15. Heinz FX, Stiasny K. 2017. The Antigenic Structure of Zika Virus and Its Relation to Other Flaviviruses: Implications for Infection and Immunoprophylaxis. Microbiol Mol Biol Rev 81.

16. Yu IM, Zhang W, Holdaway HA, Li L, Kostyuchenko VA, Chipman PR, Kuhn RJ, Rossmann MG, Chen J. 2008. Structure of the immature dengue virus at low pH primes proteolytic maturation. Science 319:1834-7.
17. Stadler K, Allison SL, Schalich J, Heinz FX. 1997. Proteolytic activation of tick-borne encephalitis virus by furin. J Virol 71:8475-81.
18. Harrison SC. 2015. Viral membrane fusion. Virology 479-480:498-507.
19. Rey FA, Stiasny K, Vaney MC, Dellarole M, Heinz FX. 2018. The bright and the dark side of human antibody responses to flaviviruses: lessons for vaccine design. EMBO Rep 19:206-224.
20. Dejnirattisai W, Supasa P, Wongwiwat W, Rouvinski A, Barba-Spaeth G, Duangchinda T, Sakuntabhai A, Cao-Lormeau VM, Malasit P, Rey FA, Mongkolsapaya J, Screaton GR. 2016. Dengue virus sero-cross-reactivity drives antibody-dependent enhancement of infection with zika virus. Nat Immunol 17:1102-8.
21. Beltramello M, Williams KL, Simmons CP, Macagno A, Simonelli L, Quyen NT, Sukupolvi-Petty S, Navarro-Sanchez E, Young PR, de Silva AM, Rey FA, Varani L, Whitehead SS, Diamond MS, Harris E, Lanzavecchia A, Sallusto F. 2010. The human immune response to Dengue virus is dominated by highly cross-reactive antibodies endowed with neutralizing and enhancing activity. Cell Host Microbe 8:271-83.
22. Dejnirattisai W, Jumnainsong A, Onsirisakul N, Fitton P, Vasanawathana S, Limpitikul W, Puttikhunt C, Edwards C, Duangchinda T, Supasa S, Chawansuntati K, Malasit P, Mongkolsapaya J, Screaton G. 2010. Cross-reacting antibodies enhance dengue virus infection in humans. Science 328:745-8.
23. de Alwis R, Smith SA, Olivarez NP, Messer WB, Huynh JP, Wahala WM, White LJ, Diamond MS, Baric RS, Crowe JE, Jr., de Silva AM. 2012. Identification of human neutralizing antibodies that bind to complex epitopes on dengue virions. Proc Natl Acad Sci U S A 109:7439-44.
24. Dejnirattisai W, Wongwiwat W, Supasa S, Zhang X, Dai X, Rouvinski A, Jumnainsong A, Edwards C, Quyen NTH, Duangchinda T, Grimes JM, Tsai WY, Lai CY, Wang WK, Malasit P, Farrar J, Simmons CP, Zhou ZH, Rey FA, Mongkolsapaya J, Screaton GR. 2015. A new class of highly potent, broadly neutralizing antibodies isolated from viremic patients infected with dengue virus. Nat Immunol 16:170-177.
25. Barba-Spaeth G, Dejnirattisai W, Rouvinski A, Vaney MC, Medits I, Sharma A, Simon-Loriere E, Sakuntabhai A, Cao-Lormeau VM, Haouz A, England P, Stiasny K, Mongkolsapaya J, Heinz FX, Screaton GR, Rey FA. 2016. Structural basis of potent Zika-dengue virus antibody cross-neutralization. Nature 536:48-53.
26. Swanstrom JA, Plante JA, Plante KS, Young EF, McGowan E, Gallichotte EN, Widman DG, Heise MT, de Silva AM, Baric RS. 2016. Dengue Virus Envelope Dimer Epitope Monoclonal Antibodies Isolated from Dengue Patients Are Protective against Zika Virus. MBio 7.
27. Fernandez E, Dejnirattisai W, Cao B, Scheaffer SM, Supasa P, Wongwiwat W, Esakky P, Drury A, Mongkolsapaya J, Moley KH, Mysorekar IU, Screaton GR, Diamond MS. 2017. Human antibodies to the dengue virus E-dimer epitope have therapeutic activity against Zika virus infection. Nat Immunol 18:1261-1269.
28. Slon Campos JL, Marchese S, Rana J, Mossenta M, Poggianella M, Bestagno M, Burrone OR. 2017. Temperature-dependent folding allows stable dimerization of secretory and virus-associated E proteins of Dengue and Zika viruses in mammalian cells. Sci Rep 7:966.
29. Sirohi D, Chen Z, Sun L, Klose T, Pierson TC, Rossmann MG, Kuhn RJ. 2016. The 3.8 A resolution cryo-EM structure of Zika virus. Science 352:467-70.
30. Rossi SL, Tesh RB, Azar SR, Muruato AE, Hanley KA, Auguste AJ, Langsjoen RM, Paessler S, Vasilakis N, Weaver SC. 2016. Characterization of a Novel Murine Model to Study Zika Virus. Am J Trop Med Hyg 94:1362-1369.

Journal of Virology

31. Dowall SD, Graham VA, Rayner E, Hunter L, Atkinson B, Pearson G, Dennis M, Hewson R. 2017. Lineage-dependent differences in the disease progression of Zika virus infection in type-I interferon receptor knockout (A129) mice. PLoS Negl Trop Dis 11:e0005704.
32. Poggianella M, Slon Campos JL, Chan KR, Tan HC, Bestagno M, Ooi EE, Burrone OR. 2015. Dengue E Protein Domain III-Based DNA Immunisation Induces Strong Antibody Responses to All Four Viral Serotypes. PLoS Negl Trop Dis 9:e0003947.
33. Predonzani A, Arnoldi F, Lopez-Requena A, Burrone OR. 2008. In vivo site-specific biotinylation of proteins within the secretory pathway using a single vector system. BMC Biotechnol 8:41.
34. Dowall SD, Graham VA, Rayner E, Atkinson B, Hall G, Watson RJ, Bosworth A, Bonney LC, Kitchen S, Hewson R. 2016. A Susceptible Mouse Model for Zika Virus Infection. PLoS Negl Trop Dis 10:e0004658.
35. Fibriansah G, Tan JL, Smith SA, de Alwis R, Ng TS, Kostyuchenko VA, Jadi RS, Kukkaro P, de Silva AM, Crowe JE, Lok SM. 2015. A highly potent human antibody neutralizes dengue virus serotype 3 by binding across three surface proteins. Nat Commun 6:6341.
36. Fibriansah G, Tan JL, Smith SA, de Alwis AR, Ng TS, Kostyuchenko VA, Ibarra KD, Wang J, Harris E, de Silva A, Crowe JE, Jr., Lok SM. 2014. A potent anti-dengue human antibody preferentially recognizes the conformation of E protein monomers assembled on the virus surface. EMBO Mol Med 6:358-71.
37. Stettler K, Beltramello M, Espinosa DA, Graham V, Cassotta A, Bianchi S, Vanzetta F, Minola A, Jaconi S, Mele F, Foglierini M, Pedotti M, Simonelli L, Dowall S, Atkinson B, Percivalle E, Simmons CP, Varani L, Blum J, Baldanti F, Cameroni E, Hewson R, Harris E, Lanzavecchia A, Sallusto F, Corti D. 2016. Specificity, cross-reactivity, and function of antibodies elicited by Zika virus infection. Science 353:823-6.
38. Kudlacek ST, Premkumar L, Metz SW, Tripathy A, Bobkov AA, Payne AM, Graham S, Brackbill JA, Miley MJ, de Silva AM, Kuhlman B. 2018. Physiological temperatures reduce dimerization of dengue and Zika virus recombinant envelope proteins. J Biol Chem 293:8922-8933.
39. Yang C, Zeng F, Gao X, Zhao S, Li X, Liu S, Li N, Deng C, Zhang B, Gong R. 2019. Characterization of two engineered dimeric Zika virus envelope proteins as immunogens for neutralizing antibody selection and vaccine design. J Biol Chem 294:10638-10648.
40. Slon-Campos JL, Dejnirattisai W, Jagger BW, Lopez-Camacho C, Wongwiwat W, Durnell LA, Winkler ES, Chen RE, Reyes-Sandoval A, Rey FA, Diamond MS, Mongkolsapaya J, Screaton GR. 2019. A protective Zika virus E-dimer-based subunit vaccine engineered to abrogate antibody-dependent enhancement of dengue infection. Nat Immunol doi:10.1038/s41590-019-0477-z.
41. Metz SW, Thomas A, Brackbill A, Forsberg J, Miley MJ, Lopez CA, Lazear HM, Tian S, de Silva AM. 2019. Oligomeric state of the ZIKV E protein defines protective immune responses. Nat Commun 10:4606.
42. Kostyuchenko VA, Lim EX, Zhang S, Fibriansah G, Ng TS, Ooi JS, Shi J, Lok SM. 2016. Structure of the thermally stable Zika virus. Nature 533:425-8.
43. Smith SA, Nivarthi UK, de Alwis R, Kose N, Sapparapu G, Bombardi R, Kahle KM, Pfaff JM, Lieberman S, Doranz BJ, de Silva AM, Crowe JE, Jr. 2016. Dengue Virus prM-Specific Human Monoclonal Antibodies with Virus Replication-Enhancing Properties Recognize a Single Immunodominant Antigenic Site. J Virol 90:780-9.
44. Priyamvada L, Quicke KM, Hudson WH, Onlamoon N, Sewatanon J, Edupuganti S, Pattanapanyasat K, Chokephaibulkit K, Mulligan MJ, Wilson PC, Ahmed R, Suthar MS, Wrammert J. 2016. Human antibody responses after dengue virus infection are highly cross-reactive to Zika virus. Proc Natl Acad Sci U S A 113:7852-7.
45. Bardina SV, Bunduc P, Tripathi S, Duehr J, Frere JJ, Brown JA, Nachbagauer R, Foster GA, Krysztof D, Tortorella D, Stramer SL, Garcia-Sastre A, Krammer F, Lim JK. 2017. Enhancement of Zika virus pathogenesis by preexisting antiflavivirus immunity. Science 356:175-180.

46. Willis E, Hensley SE. 2017. Characterization of Zika virus binding and enhancement potential of a large panel of flavivirus murine monoclonal antibodies. Virology 508:1-6.
47. Pantoja P, Perez-Guzman EX, Rodriguez IV, White LJ, Gonzalez O, Serrano C, Giavedoni L, Hodara V, Cruz L, Arana T, Martinez MI, Hassert MA, Brien JD, Pinto AK, de Silva A, Sariol CA. 2017. Zika virus pathogenesis in rhesus macaques is unaffected by pre-existing immunity to dengue virus. Nat Commun 8:15674.
48. Gordon A, Gresh L, Ojeda S, Katzelnick LC, Sanchez N, Mercado JC, Chowell G, Lopez B, Elizondo D, Coloma J, Burger-Calderon R, Kuan G, Balmaseda A, Harris E. 2019. Prior dengue virus infection and risk of Zika: A pediatric cohort in Nicaragua. PLoS Med 16:e1002726.
49. Duehr J, Lee S, Singh G, Foster GA, Krysztof D, Stramer SL, Bermudez Gonzalez MC, Menichetti E, Geretschlager R, Gabriel C, Simon V, Lim JK, Krammer F. 2018. Tick-Borne Encephalitis Virus Vaccine-Induced Human Antibodies Mediate Negligible Enhancement of Zika Virus Infection InVitro and in a Mouse Model. mSphere 3.
50. Luppe MJ, Verro AT, Barbosa AS, Nogueira ML, Undurraga EA, da Silva NS. 2019. Yellow fever (YF) vaccination does not increase dengue severity: A retrospective study based on 11,448 dengue notifications in a YF and dengue endemic region. Travel Med Infect Dis doi:10.1016/j.tmaid.2019.05.002.
51. Katzelnick LC, Narvaez C, Arguello S, Lopez Mercado B, Collado D, Ampie O, Elizondo D, Miranda T, Bustos Carillo F, Mercado JC, Latta K, Schiller A, Segovia-Chumbez B, Ojeda S, Sanchez N, Plazaola M, Coloma J, Halloran ME, Premkumar L, Gordon A, Narvaez F, de Silva AM, Kuan G, Balmaseda A, Harris E. 2020. Zika virus infection enhances future risk of severe dengue disease. Science 369:1123-1128.
52. Lopez-Camacho C, De Lorenzo G, Slon-Campos JL, Dowall S, Abbink P, Larocca RA, Kim YC, Poggianella M, Graham V, Findlay-Wilson S, Rayner E, Carmichael J, Dejnirattisai W, Boyd M, Hewson R, Mongkolsapaya J, Screaton GR, Barouch DH, Burrone OR, Patel AH, Reyes-Sandoval A. 2020. Immunogenicity and Efficacy of Zika Virus Envelope Domain III in DNA, Protein, and ChAdOx1 Adenoviral-Vectored Vaccines. Vaccines (Basel) 8.
53. Donald CL, Brennan B, Cumberworth SL, Rezelj VV, Clark JJ, Cordeiro MT, Freitas de Oliveira Franca R, Pena LJ, Wilkie GS, Da Silva Filipe A, Davis C, Hughes J, Varjak M, Selinger M, Zuvanov L, Owsianka AM, Patel AH, McLauchlan J, Lindenbach BD, Fall G, Sall AA, Biek R, Rehwinkel J, Schnettler E, Kohl A. 2016. Full Genome Sequence and sfRNA Interferon Antagonist Activity of Zika Virus from Recife, Brazil. PLoS Negl Trop Dis 10:e0005048.

829 **Figure Legends**

830

831 **Figure 1: Expression, purification and characterisation of ZIKV E antigens.** (**A)**
832 Schematics of the genetic constructs used to express SV5-tagged ZIKV sE (amino
833 acid or aa 1 – 404) in the WT or cvD (carrying A264C mutation) form. Expi293F cells
834 were transiently transfected with the relevant constructs and the expressed proteins
835 secreted into the medium were purified using V5-tag affinity chromatography. (**B)**
836 **SDS-PAGE of the purified protein.** sE-WT and sE-cvD were analysed in SDS-
837 PAGE run in presence or absence of reducing conditions. Black arrows show
838 monomers of sE, blue arrows show dimers. (**C) Schematics of VLP antigens**
839 **design and purification:** Plasmid constructs carrying the sequences encoding the
840 capsid anchor (i.e. the N-terminal 18 amino acids of Capsid protein), followed by prM
841 and full-length E genes, the latter in its WT form or in the form of cvD (i.e. carrying
842 the A264C mutation). The constructs were transiently transfected in Expi293F cells
843 and the secreted VLPs were pelleted by sucrose cushion 4 days post-transfection
844 and subsequently purified by density gradient followed by size-exclusion
845 chromatography (SEC). (**D) Western Blot of the purified VLPs showing dimeric**
846 **conformation:** Purified VLP-WT and VLP-cvD were analysed by SDS-PAGE under
847 reducing or non-reducing conditions E was detected using in-house made
848 monoclonal antibody DIII-1B. Black arrows show E monomers; blue arrow shows
849 dimers; grey arrows show higher order oligomers (non-reducing gel) or partially
850 resolved complexes (reducing gel) of the E protein. **(E) Western Blot of the purified**
851 **VLPs showing prM and M content:** Purified VLP-WT and VLP-cvD were analysed
852 by SDS-PAGE (14% acrylamide) under reducing conditions. Protein E was detected
853 using the monoclonal antibody DIII-1B (in green), whereas proteins prM and M were

854 detected using an anti-M antibody (in red). (**F) Electron microscope picture of**
855 **purified VLPs:** Electron microscopy (uranyl acetate staining) of VLP-WT (left panel)
856 and VLP-cvD (right panel) purified as described in (c). Bars indicate the diameter of
857 the particles.
858
859 **Figure 2:** (**A) Schematic representation of the immunisation procedure:** Five
860 groups each (n=6) of 4 weeks-old mice received respectively sE-WT, sE-cvD, VLP-
861 WT, VLP-cvD or PBS, mixed with ALUM-MPLA adjuvant as shown. Following two
862 boosts at weeks 2 and 3, test bleeds were collected at week 4 for analyses. (**B and**
863 **C) Anti-E antibody titres of sera collected from animals immunised with sE (B)**
864 **or VLP proteins (C).** Antibody titres were determined using ELISA plates coated
865 with mono-biotinylated monomeric E, dimeric E and DIII. Ctrl: pooled sera from PBS
866 control group. The titre was defined as the maximum dilution that gives a value
867 higher than three-times the value given by the pre-immune sera. The control sera
868 were negative at the lowest dilution (1:900) and their titre was calculated as 1/3 of
869 that dilution (300). Statistical analysis was done using 2-sided ANOVA 95%
870 confidence level with Tukey Pairwise comparison at 95% confidence (Minitab
871 software).
872
873 **Figure 3: Determination of binding characteristics of serum IgGs to different**
874 **sE conformations**. Cells expressing sE on the cell surface were incubated with **(A)**
875 pooled control sera (Control), monoclonal EDE antibody 1C10 (EDE), monoclonal
876 DIII-1B antibody (DIII-1B) at pH 6.0 (red) or pH 7.0 (blue). Following washing, the
877 bound antibodies were detected using a fluorescence-tagged secondary antibody
878 and the relative fluorescence determined by flow cytometry using FACSCalibur.

879 Mean of fluorescence intensity was calculated using FlowJo software and plotted
880 (fourth panel). (**B and C**) Sera from immunised animals were incubated with cells as
881 described in A. (**B**) Histogram plots show data of one serum as representative of
882 each immunised group. **(C)** Bar charts showing data of sera from individual animals
883 from each immunised group plotted as mean of fluorescence intensity. **D**) Ratio
884 between the intensity of fluorescence at different pH was calculated, grey column
885 represent mean. Statistical analysis was done using one-way ANOVA 95%
886 confidence level with Tukey's multiple comparison (GraphPad software). Data are
887 representative of three independent experiments, performed with pooled and single
888 sera. **Characterisation of the mouse monoclonal antibody (MAb) DIII-1B.** MAb
889 DIII-1B was obtained using standard hybridomas technology from Balb/c immunised
890 with recombinant domain III of ZIKV E protein. The specificity of MAb DIII-1B was
891 tested by **(E)** western immunoblotting of VERO cells that were mock-infected (-) or
892 infected with ZIKV (+). As expected, MAb DIII-1B specifically bound to ZIKV E
893 protein. Protein molecular weight ladder is shown on the left in kDa. Separately, the
894 binding specificity of MAb DIII-1B was also tested by **(F)** indirect
895 immunofluorescence of uninfected or ZIKV-infected A549-NPro cells. Green signal
896 indicates antibody binding to ZIKV E protein. Cell nuclei were stained with DAPI
897 (blue).
898
899 **Figure 4: Determination of anti-E or neutralising antibody titres of sera from**
900 **vaccinated animals. (A) Anti-E titres:** ELISA plates coated with biotinylated
901 dimeric E were incubated with serially diluted serum samples and the bound
902 antibodies detected as described in Materials and Methods. Antibody titres were
903 determined as described in the Figure 2 legend. (**B) Neutralisation of ZIKV**

infection: Serially diluted samples of mouse sera were incubated with ZIKV for 1 hour before infecting Vero cells. At 72 hours post-infection, the intracellular levels of E were determined by capture sandwich ELISA and percentage of infectivity relative to the virus alone infection was calculated. The results were plotted as MN_{50} values - i.e. titres at which 50% neutralisation was achieved. Statistical analysis was performed using 2-sided ANOVA 95% confidence level with Tukey Pairwise comparison at 95% confidence (Minitab software). Data from three independent experiments were used

Figure 5: *In vivo* efficacy of candidate vaccines. (A) Schematic representation of the *in vivo* challenge protocol: Mice were challenged with 10^4 pfu of ZIKV PRVABC59 one month after the primary immunisation and were monitored for up to 9 days. Test bleeds (TB) and organs were collected as shown. **Animals were weighed (C) and scored for clinical signs daily post-challenge with percentage of survival shown in (B). (D)** Legend of scoring system used to monitor animal health following ZIKV challenge**. (E)** Table showing the score attributed to each animal after ZIKV PRVABC59 challenge. Animals displaying a weight loss of 15% or more were euthanised. All the member of the control group reached the endpoint score 7-8 days post-challenge and were therefore euthanised. Statistical analysis was performed using Log-Rank (Mantel-Cox test) with GraphPad Prism software.

Figure 6: Viral titre in challenged animals. (A) The levels of ZIKV in the serum at day 2, 3, 4 and 7 post-infection were quantified by RT-qPCR and the results plotted as pfu/ml. (**B**) The limit of detection was estimated to be 100 pfu/mL, indicated by the green line. Columns show mean of all mice. Statistical significance

is reported in the table. **(C) Relative viral load in brain, spleen and sexual organs:** The presence of viral RNA in tissues was quantified by RT-qPCR and the results plotted as relative viral load calculated on the average of the PBS control group. Statistical significance is reported in the table. Statistical analysis was done using 2-sided ANOVA 95% confidence level with Tukey Pairwise comparison at 95% confidence with Minitab software.

Figure 7: Effect of pooled sera on ADE of infection by all four DENV serotypes 1-4, ZIKV, WNV and YFV. Viruses were pre-incubated with 10-fold dilution of pooled sera for 1 hour before infecting K562 cells. Percentage of infected cells was calculated by cytofluorimetry. Control consists of pooled sera from PBS-injected mice. Statistical significance applies to the comparison between VLP-WT and sE-cvD/VLP-cvD. Statistical analysis was done using 2-sided ANOVA 95% confidence level with Tukey Pairwise multiple comparison (GraphPad software). Experiments were performed in triplicate.

Figure 8: (A) Survival rate of vaccinated animals upon ZIKV challenge: Mice were challenged with 10^4 pfu of ZIKV MP1751. All the member of the control group reached the endpoint score 6 days post-challenge and were therefore euthanised. Statistical analysis was performed using Log-Rank (Mantel-Cox test) with GraphPad Prism software. (**B) Body weight variations after challenge:** weight loss of mice after ZIKV infection. Animals showing a weight loss of 15% or higher were euthanised. **(C)** Clinical scores attributed to each animal after ZIKV MP1751 challenge. **(D) Viral load in serum:** The presence of ZIKV in the serum at day 2, 3 and 4 post-infection was quantified by RT-qPCR. Green line indicates the limit of

detection. **(E) Relative viral load in brain:** presence of viral RNA in tissues was quantified by RT-qPCR. Statistical analysis was done using 2 sided Two-Sample T-Test 95% confidence level with Minitab software.

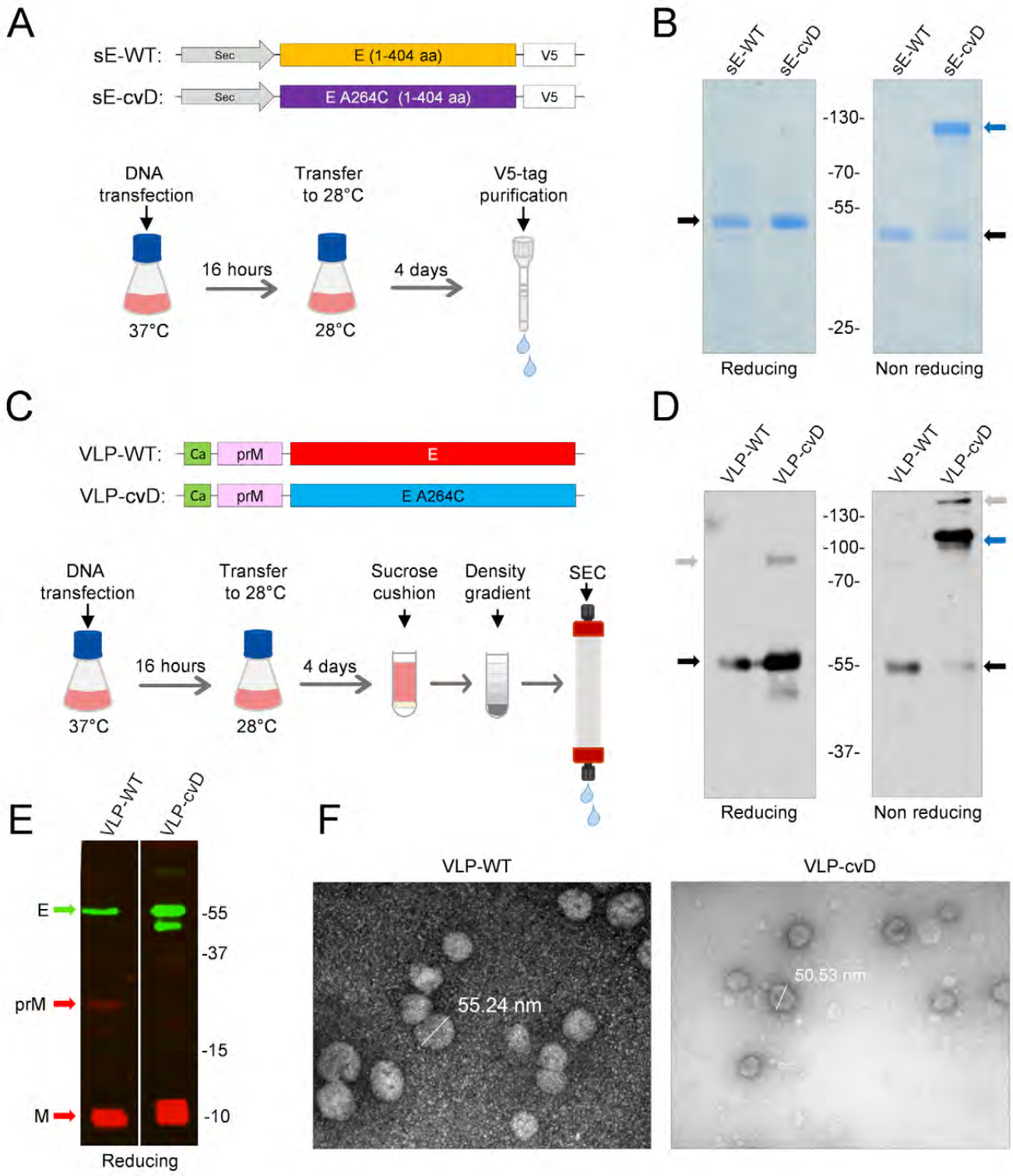

Figure 1

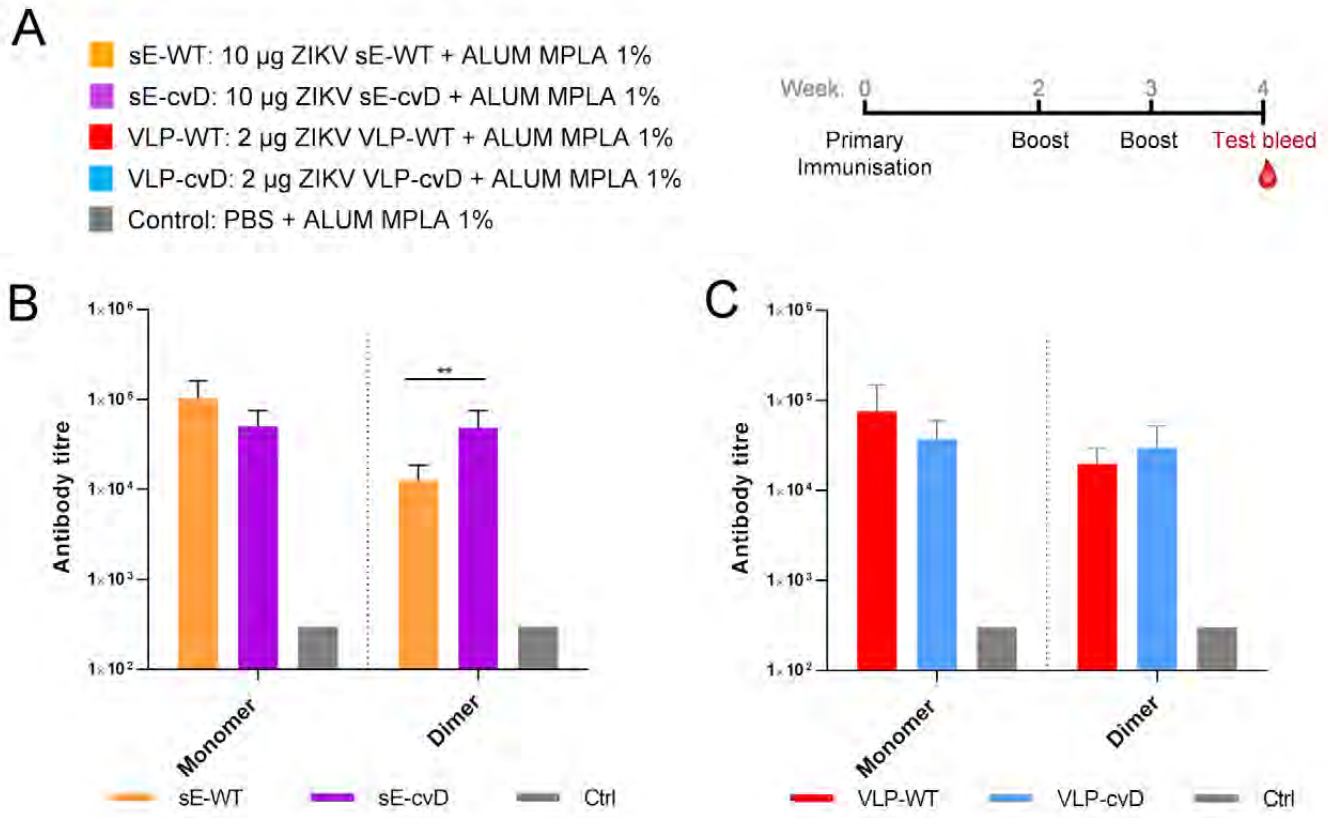

Figure 2

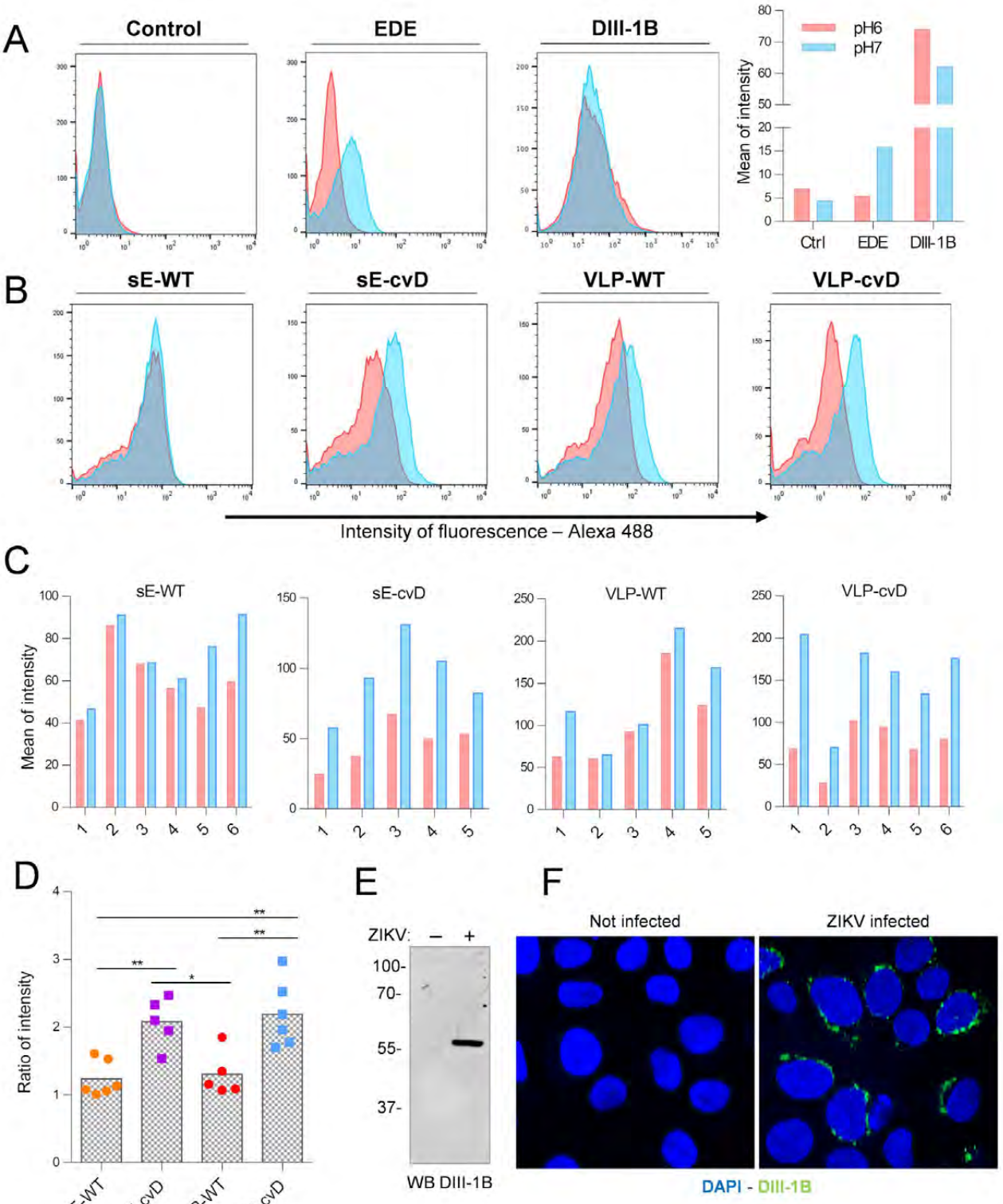

Figure 3

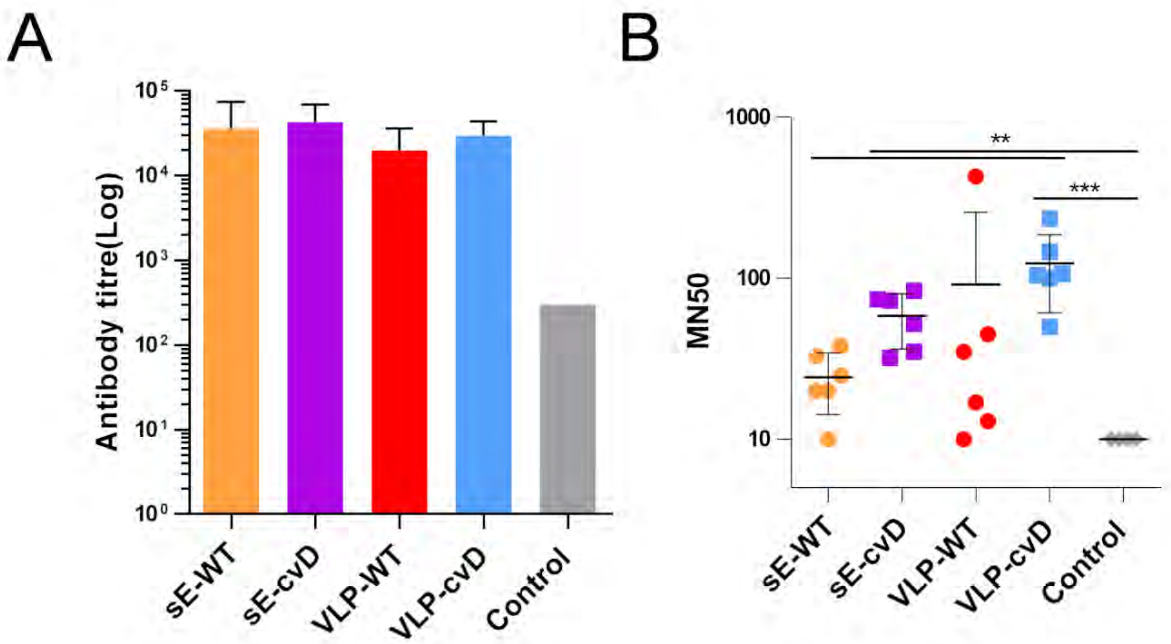

Figure 4

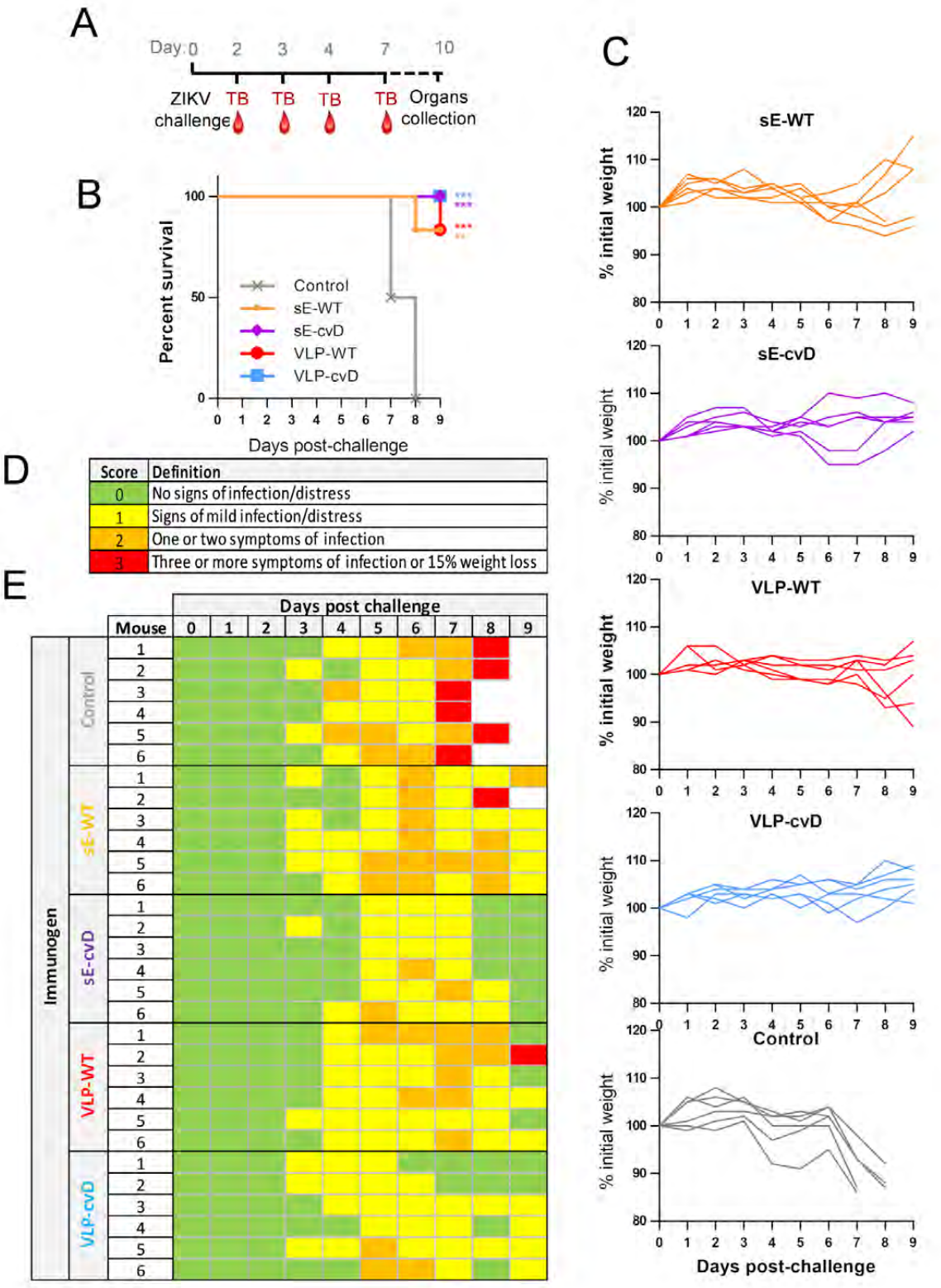

Figure 5

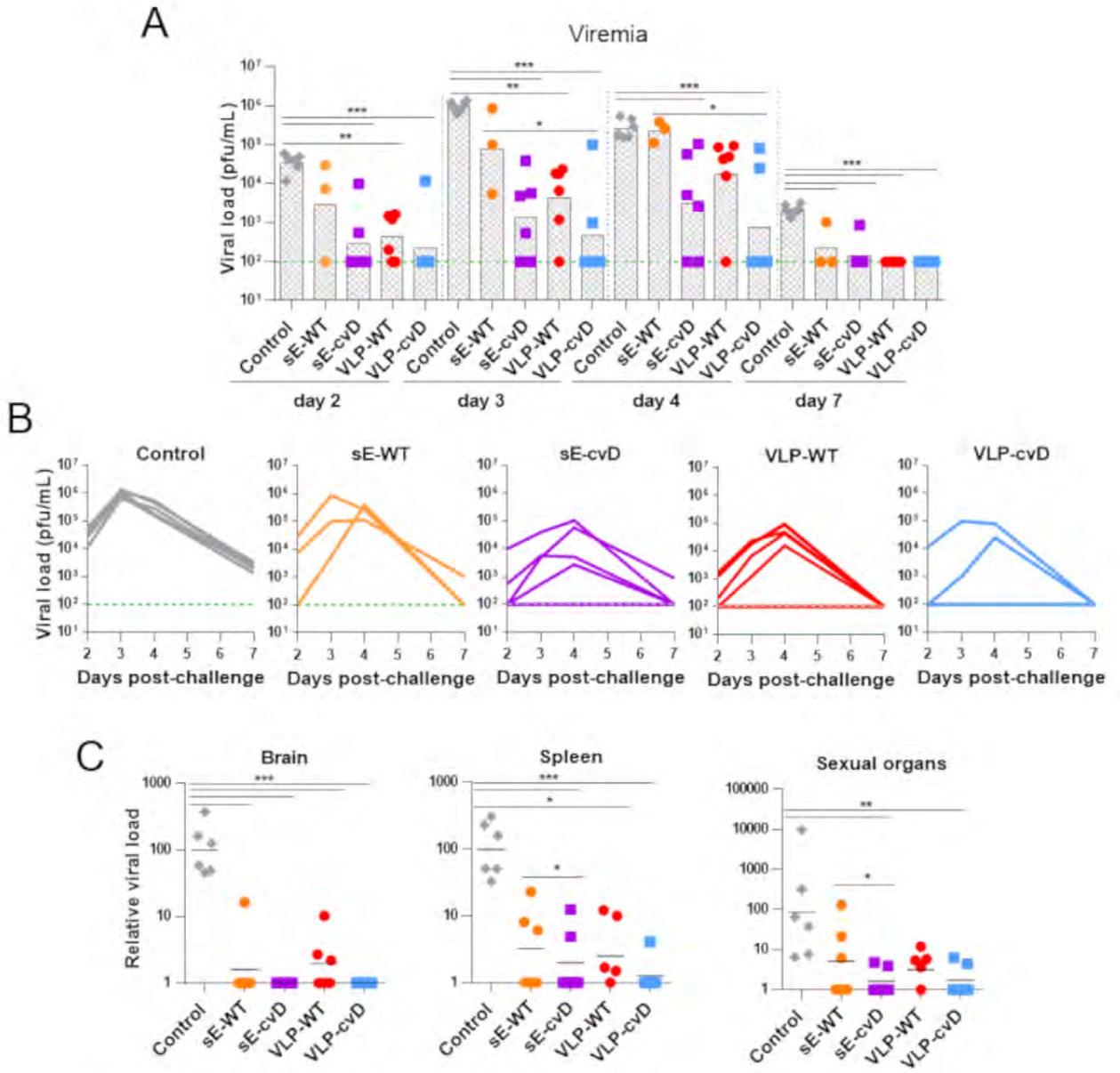

Figure 6

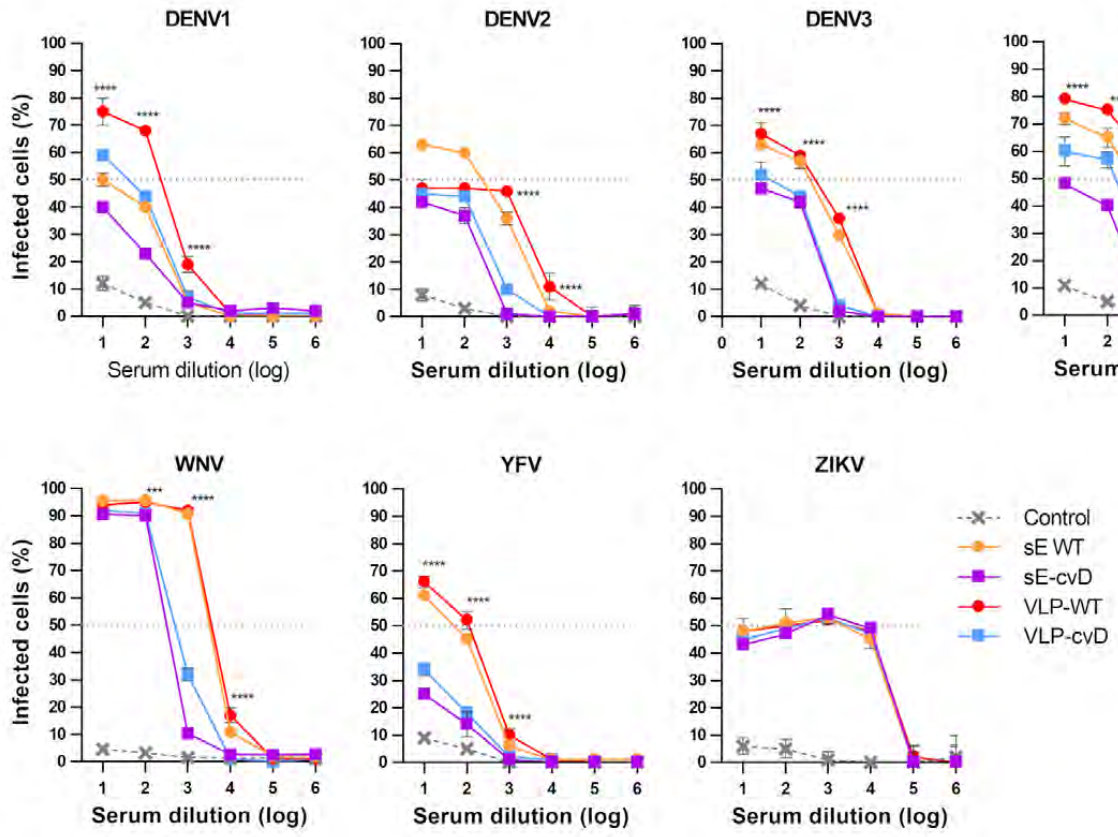

Figure 7

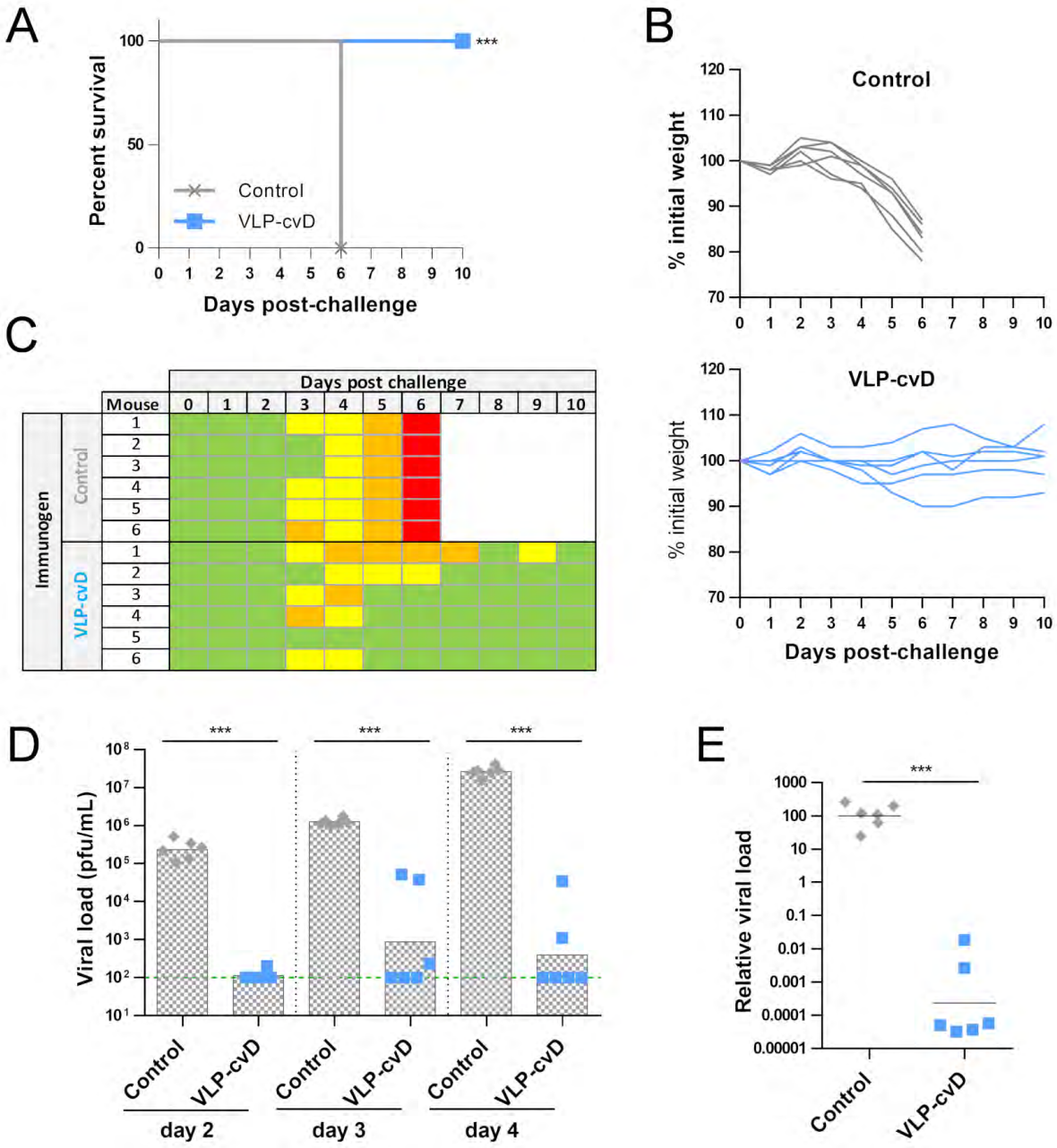

Figure 8